Journal of Medicinal Chemistry

Article

pubs.acs.org/jmc

Design, Synthesis, and Qualitative Structure–Activity Evaluations of Novel β-Secretase Inhibitors as Potential Alzheimer's Drug Leads

Taleb H. Al-Tel,*[,†] Mohammad H. Semreen,[†] Raed A. Al-Qawasmeh,[§] Marco F. Schmidt,[∥] Raafat El-Awadi,[†] Mustafa Ardah,[⊥] Rania Zaarour,[‡] Shashidhar N. Rao,[#] and Omar El-Agnaf[⊥]

[†]College of Pharmacy and [‡]Sharjah Institute for Medical Research, University of Sharjah, P.O. Box 27272, Sharjah, UAE

[§]Chemistry Department, University of Jordan, 11942, Amman, Jordan

[∥]University Chemical Laboratory, University of Cambridge, Lensfield Road, Cambridge CB2 EW1, U.K.

[⊥]Faculty of Medicine & Health Sciences, United Arab Emirates University, P.O. Box 17666 Al-Ain, UAE

[#]Tripos International, Inc., 1699 South Hanley Road, St. Louis, Missouri 63144, United States

Supporting Information

ABSTRACT: We have identified highly selective imidazopyridines armed with benzimidazol and/or arylimidazole as potent β-secretase inhibitors. The most effective and selective analogues demonstrated low nanomolar potency for the BACE1 enzyme as measured by FRET and cell-based (ELISA) assays and exhibited comparable affinity (K_I) and high ligand efficiency (LE). In addition, these motifs were highly selective (>200) against the structurally related aspartyl protease BACE2. Our design strategy followed a traditional SAR approach and was supported by molecular modeling studies based on the previously reported hydroxyethylene transition state inhibitor derived from isophthalic acid **I**. Of the most potent compounds, **34** displayed an IC_{50} for BACE1 of 18 nM and exhibited cellular activity with an EC_{50} of 37 nM in the cell-based ELISA assay, as well as high affinity (K_I = 17 nM) and ligand efficiency (LE = 1.7 kJ/mol). Compound **34** was found to be 204-fold more selective for BACE1 compared to the closely related aspartyl protease BACE2.

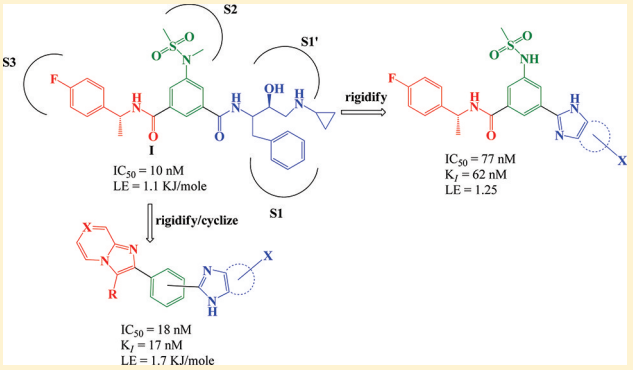

INTRODUCTION

Alzheimer's disease (AD) is the most common form of irreversible dementia.[1] More than 25 million people are suffering from dementia, and the annual socioeconomic worldwide costs have been estimated to exceed U.S. $200 billion.[1] According to the Alzheimer's Association, in 2009 an estimated 5.3 million Americans had Alzheimer's disease (AD), making it the sixth leading cause of death in the United States. As increased age is the major risk factor of the disease, AD frequency is expected to increase to an estimated 7.7 million cases in 2030 and 11–16 million cases in 2050 in the United States alone. These numbers do not encompass the large number of people with mild cognitive impairment, a considerable proportion of whom will progress to AD.[2] Genetic and pathological evidence strongly supports the amyloid cascade hypothesis for AD. This states that Aβ, a proteolytic derivative of the large transmembrane amyloid precursor protein (APP), in particular the least soluble 42 amino acid fragment Aβ42 isoform, has an early and imperative role in all forms of AD.[3]

To date, treatment of AD only partly reduces the symptoms and does not affect the underlying progression of the disease.[4] The accumulation and aggregation of extracellular Aβ plaques in the brain is a hallmark of AD.[5] Thus, the most direct approach in AD therapy is the reduction of Aβ42 production. Aβ is generated proteolytically from a large precursor molecule, APP, by the sequential action of two proteases: β-secretase (also known as β-site APP cleaving enzyme 1, BACE1) and γ-secretase. A third protease, α-secretase, competes with β-secretase for the APP substrate and can prevent the production of Aβ by cleaving the peptide into two fragments. These molecular pathways evoke at least three strategies to reduce Aβ: inhibition of γ-secretase, inhibition of β-secretase, and stimulation of α-secretase. The main approach for targeting Aβ production involves targeting β-secretase.[6]

Tissue culture and animal studies have shown that β-secretase is expressed in all tissues, with higher expression levels in the brain. Enhanced β-secretase activity has been detected in the brains of patients with sporadic AD.[7] Furthermore, BACE1 knockout mice are scarce in Aβ production, demonstrating that there are no redundant molecular mechanisms for β-secretase cleavage in mice. More interestingly, the knockout mice did not manifest severe health defects as a result of the lack of β-secretase;

Received: June 17, 2011
Published: November 1, 2011

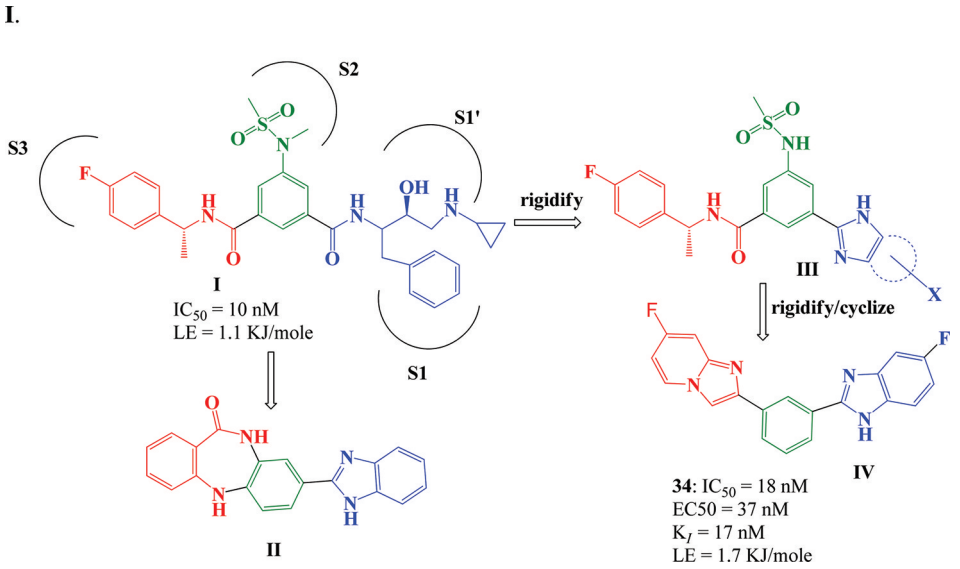

Figure 1. De novo design strategies utilized to find P1−P1′ and P3 fragments based on isophthalic acid motif **I**.

they had no aberrant phenotype and were fertile, and clinical chemistry parameters were normal in both young and old animals. Both the absence of Aβ production and the lack of distinct pathology of the BACE1 knockout mice emphasized the potential effectiveness of drugs targeting β-secretase. However, the development of specific inhibitors for β-secretase has proven to be highly challenging.[8]

To date, one company has reported clinical data with γ-secretase inhibitor, and over the past 2 decades many groups and Biotech Pharma have investigated a diversity of approaches to the design of BACE1 inhibitors.[9] These efforts have produced low molecular weight BACE1 inhibitors with little or no peptidic character.[10] In addition, recent reports have revealed the application of fragment-based lead generation approaches as an alternative route to the design of potent small-molecule BACE1 inhibitors.[11] The discovery of low molecular weight BACE1 inhibitors has also led to the improvement of the physicochemical properties of the compounds as verified by their high-permeability in cell-based assays.[12]

BACE2 is a closely related aspartyl protease. The physiological functions of BACE2 have to be fully characterized, although BACE1/BACE2 double knockout mice have been reported to be viable.[13]

RESULTS AND DISCUSSION

We have previously reported on the design and synthesis of benzodiazepine motifs of type **II** (Figure 1) as potential lead molecules for BACE1 inhibition.[14] As a continuation of this work, we report herein on the design and synthesis of novel motifs derived from isophthalic and terephthalic acid as potential BACE1 inhibitors. As could be concluded from Figure 1, we followed a traditional medicinal chemistry strategy, namely, extension/contraction, rigidification/cyclization, positional ring variations, and bioisostere replacement, to arrive at our intended motifs. In this respect, we considered the extensive structure−activity relationship (SAR) investigations presented in our previous article.[14] We learned that the truncation of the benzimidazole segment (benzodiazepine derivatives of type **II**, Figure 1) as an isostere of the amide handle of compound **I** led to more rigid and potent motifs that possessed an IC_{50} of about 200 nM against BACE1.[14] Thus, we decided to replace the hydroxyethylene (HE) amide portion of compound **I** with benzimidazole and/or arylimidazole derivatives, leading to compounds of type **III**. We hypothesized that this might improve the affinity of such motifs against BACE1. Accordingly, the IC_{50} of such motifs (**6**−**8** and **12**−**14**) ranged from 1.08 to 0.187 μM (Tables 1 and 2). The results were promising. However, such series displayed high polar surface area (PSA), an indication of low oral bioavailability,[15] and a high peptidic nature; hence, we decided to design more rigid motifs to lower the peptidic portions and the PSA. We therefore carried out detailed SAR studies around compounds **II** and **III** that ultimately led us to contract the diazepam ring, leading to imidazopyridine derivative of type **IV**. This resulted in some cases of up to 60-fold improvement of the ligand affinity (**34** vs **6**) toward BACE1 enzyme (**34**, IC_{50} = 18 nM; Table 5) and comparable activity in the cell-based ELISA assay (EC_{50} = 37 nM). In addition, compound **34** demonstrated about 204-fold selectivity against the closely related aspartyl protease, BACE2, and its solubility in water was 10 mg/mL. Furthermore, we found that linear terephthalic acid like scaffolds (e.g., **19**−**21**) on the targeted ligand at the vicinity of this aberration generated steric conflict between the ligand and this protein, thus impacting the ligand's affinity and efficiency. These results were in contrast to the isophthalic acid like motifs (e.g., **24**−**26** and **31**−**34**), which lacked such steric compression and exhibited high protein affinity.

Synthesis. The preparation of the compounds needed to delineate the SAR for this study was done according to synthetic Schemes 1 and 2. Two types of scaffolds were synthesized. In the first, sulfone amide carboxylic acid **2**, synthesized using well established procedures,[16] was coupled with the desired diaminobenzene, **3**−**5** (Scheme 1). Thus, treatment of **2** with TBTU and DIPEA in DMF at 0 °C followed by the addition of the desired diaminobenzene (**3**, **4**, or **5**) and subsequent reaction with NH_4OAc followed by silica gel chromatography furnished compounds **6**−**8** in fairly good yields. In the second approach, compound **2** (Scheme 2) was coupled with the desired α-bromoketone **9**−**11** using DIPEA in DMF at 0 °C. Subsequently, the product from this step was subjected to cyclization reaction with the amidic carbonyl group in refluxing acetic acid to deliver compounds **12**−**14**.

dx.doi.org/10.1021/jm201181f|J. Med. Chem. 2011, 54, 8373−8385

Table 1. SAR of BACE1 Inhibitors[a]

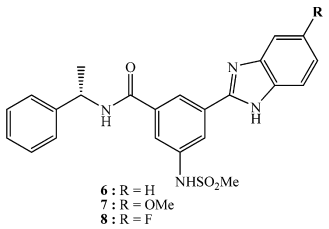

	BACE1					BACE2	
compd	IC_{50} (nM)	K_I (nM)	ELISA EC_{50} (nM)	LE (kJ/mol)	*t*PSA (Å^2)	IC_{50} (nM)	K_I (nM)
6	1080 ± 303	1041 ± 342	NA	1.07	90.9	2130	2067
7	545 ± 63	525 ± 82	NA	1.05	100.1	2425	2354
8	786 ± 262	758 ± 254	230 ± 54	1.06	90.9	2127	2065

[a]IC_{50} and EC_{50} values are the mean values of at least three experiments ± SD. NA means not applicable.

Table 2. SAR of BACE1 Inhibitors[a]

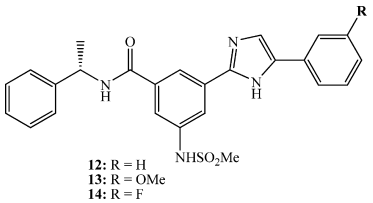

	BACE1					BACE2	
compd	IC_{50} (nM)	K_I (nM)	ELISA EC_{50} (nM)	LE (kJ/mol)	*t*PSA (Å^2)	IC_{50} (nM)	K_I (nM)
12	315 ± 112	304 ± 98	450 ± 87	1.09	90.9	1786	1733
13	77 ± 11	62 ± 13	179 ± 36	1.25	100.1	2350	2281
14	187 ± 21	180 ± 27	NA	1.16	90.9	1873	1818

[a]IC_{50} and EC_{50} values are the mean values of at least three experiments ± SD. NA means not applicable.

Scheme 1. Synthesis of the First Series of BACE1 Inhibitors 6–8[a]

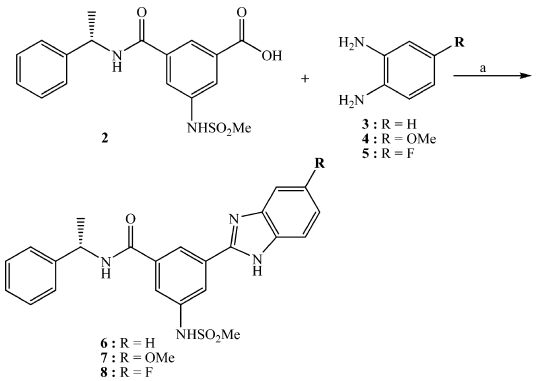

[a]Reagents and conditions: (a) TBTU, DIPEA, DMF, 0 °C, 6 h, then AcOH, reflux, 6 h.

Scheme 2. Synthesis of the Second Series of BACE1 Inhibitors 12–14[a]

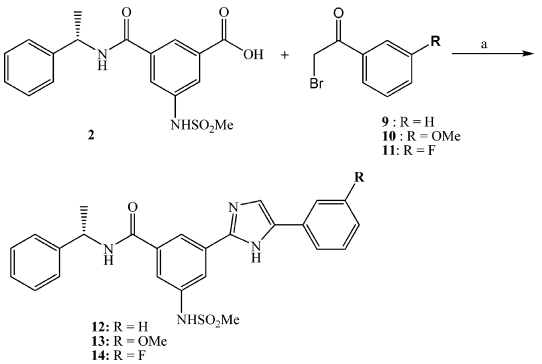

[a]Reagents and conditions: (a) DMF, DIPEA, 0 °C to room temp, 6 h (95%), then AcOH, $AcONH_4$, reflux, 8 h.

For the synthesis of the third class of compounds, namely, imidazopyridine analogues of type **19** (Scheme 3), Greobock–Blackburn [4 + 1] cycladdition protocol of aminopyridine (**15**) with phthalaldehyde **16** and isonitrile **17** was followed to afford imidazopyridine **18** in 75% yield. Without further purification, compound **18** was subjected to coupling with the desired diaminobenzene derivatives followed by acid catalyzed ring closure leading to benzimidazole derivatives **19–21**.

The fourth series of compounds (Scheme 4) were synthesized using the Greobock–Blackburn protocol as described before. Alternatively, isophthalaldehyde **22** was used in this reaction instead of terephthalic acid derivative **16**. With compound **23** in hand, it was subjected to coupling reaction with the desired diaminobenzene followed by reaction with NH_4OAc furnishing imidazopyridine motifs **24–26**. To enhance SAR diversity, 2-aminopyridine derivatives **15** and **17** (Scheme 5) were subjected to tandem coupling and cyclization reaction with *α*-bromoketone **28** to deliver adducts

dx.doi.org/10.1021/jm201181f|J. Med. Chem. 2011, 54, 8373–8385

Scheme 3. Synthesis of the Third Series of BACE1 Inhibitors 19−21[a]

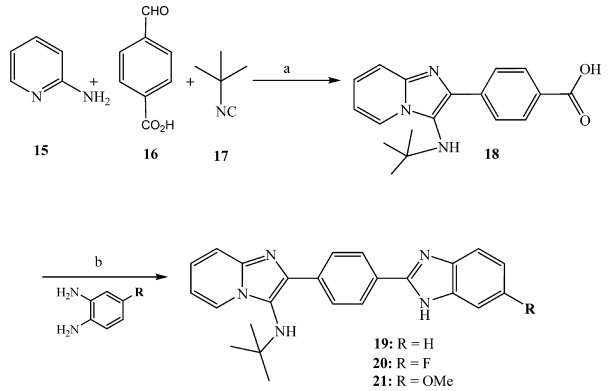

[a]Reagents and conditions: (a) $Sc(OTf)_3$, DCM−MeOH, 12 h; (b) TBTU, DIPEA, DMF, 0 °C, 6 h, then AcOH, reflux, 8 h.

Scheme 4. Synthesis of the Fourth Series of BACE1 Inhibitors 24−26[a]

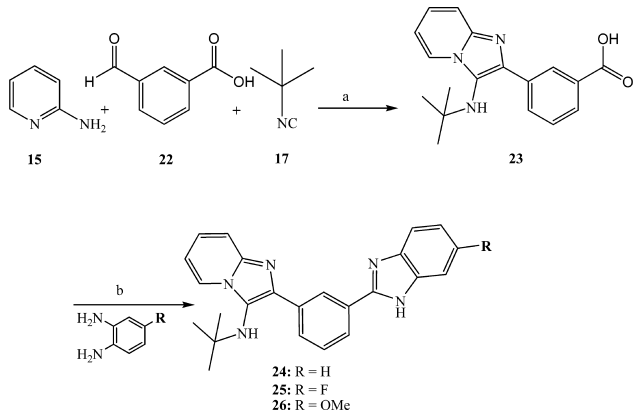

[a]Reagents and conditions: (a) $Sc(OTf)_3$, DCM−MeOH, 12 h; (b) TBTU, DIPEA, DMF, 0 °C, 6 h, then AcOH, reflux, 8 h.

Scheme 5. Synthesis of the Fifth Series of BACE1 Inhibitors 31−34[a]

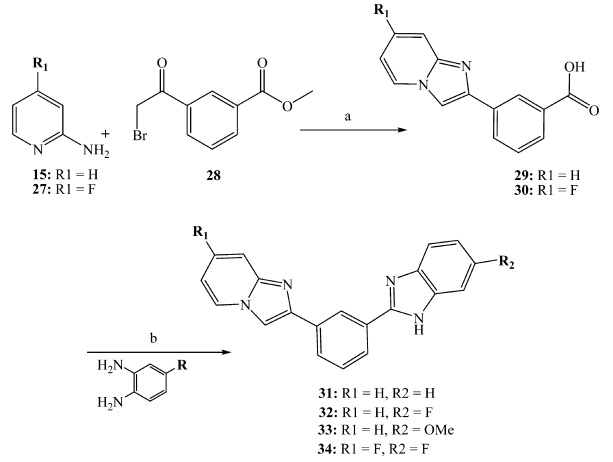

[a]Reagents and conditions: (a) EtOH, reflux 2 h, then $NaHCO_3$, reflux 12 h; (b) TBTU, DIPEA, DMF, 0 °C, 6 h, then AcOH, reflux, 8 h.

29 and **30**. These acids were coupled with the desired diaminobenzene to deliver the corresponding benzimidazole derivatives **31**−**34**. The final products were then purified using flash column chromatography, employing variable concentrations from EtOAc/DCM mixtures.

Biological Activities and SAR. Our goal in this study was to develop selective and potent BACE1 inhibitors. Toward this objective, we have first replaced the P1−P1′ portions in compound **I** by a benzimidazole arm to project directly toward the S1−S1′ subpockets of the BACE1 active site. This was initiated based on our earlier extensive SAR analysis of compound **II** (Figure 1). To prove the concept that the HE transition state mimic in compound **I** could be replaced by benzimidazole group, we have subjected compound **I** to traditional medicinal chemistry strategies leading to scaffolds such as **III** and **IV** (Figure 1). With the necessary tools needed to fully investigate the SAR in hand, the diverse array of compounds were profiled for their potency at the target enzyme BACE1, and their selectivity toward the closely related aspartyl protease BACE2 was investigated. The BACE1/BACE2 primary screening assay utilized for this program was the fluorescence resonance energy transfer (FRET) protocol. We used an APP-based peptide substrate (rhodamine-EVNLDAEFK-quencher, K_M of 20 μM) carrying the Swedish mutation and containing rhodamine as a fluorescence donor and a quencher acceptor at each end. IC_{50} values were calculated by plotting the obtained relative fluorescence unit per hour (RFU/h) against the logarithmic of inhibitor concentration. The measured inhibition data were analyzed in GraphPad Prism 4 for Windows (GraphPad Software Inc., La Jolla, CA, U.S.) by nonlinear regression (curve fitting). The observed inhibition constant in the presence of substrate, K_I (app), is calculated according to the following equation:[17]

$$\frac{v_0}{v_I} = 1 + \frac{[I]}{K_I(app)}$$

where v_I is the steady state rate of substrate hydrolysis in the presence of inhibitor concentration [I] and where v_0 is the uninhibited rate. The overall equilibrium constant is obtained taking into account the substrate concentration [S] according to the following equation:[17]

$$K_I = \frac{K_I(app)}{1 + \frac{[S]}{K_M}}$$

As an indication of the efficiency of the compounds toward binding BACE1 compared to known BACE1 inhibitors, the ligand efficiency was calculated for each compound based on the free energy equation,

$$\Delta G = -RT \ln K_I$$

and the equation of binding energy per atom (ligand efficiency, LE),

$$LE = -\Delta G/(\text{heavy atom count})$$

Cellular potency of advancing compounds was done via cell-based Aβ inhibition (Aβ40 or Aβ42) in an enzyme-linked immune sandwich assay (ELISA) in H4 cells (human neuroglioma cell line) expressing the double Swedish mutation (K595N/M596L) of human APP (APPsw). The concentration at which the cellular production of Aβ40 or Aβ42 was reduced by 50% (EC_{50}) was determined and reported in Tables 1−5.[17]

Compared to compounds **I** and **II** (Figure 1), the initial unsubstituted baseline benzimidazole analogue **6** (Table 1)

dx.doi.org/10.1021/jm201181f|J. Med. Chem. 2011, 54, 8373−8385

showed about 108-fold less in potency when compared to compound **I** (Figure 1) and a 5-fold decrease in potency when compared to the compounds of type **II**.[14] As we were not satisfied with this result, we decided to include a fluorine atom on the benzimidazole appendage. By doing so, we thought that the fluorine might be engaged in a network of hydrogen bonding in S1−S1′ subpockets leading to higher affinity.

Thus, compound **8** was synthesized according to Scheme 1 and was found to possess about 1.5-fold improvement in potency compared to compound **6**. By replacement of the fluorine atom in **8** with a methoxy group (compound **7**), the activity was enhanced by 2-fold compared to that of **6**. Compounds **7** and **8** exhibited fair selectivity (5-fold) against BACE2 and possessed modest activity against BACE 1 compared to compound **I**. Compound **8** possessed an EC_{50} of 230 nM in the cell-based ELISA assay. To understand the biological sensitivity to which compounds **6**−**8** were subject and to find a plausible explanation for the difference in the activity profiles between **6**−**8** and compound **I**, one needed to consider their docking profile in the enzyme active site in an attempt. Thus, we analyzed the X-ray cocrystal structures of BACE1 protein available in Protein Data Bank reported for compound **I** (2B8L) and used this structure to calculate the molecular modeling (Figure 2) data for our compounds using

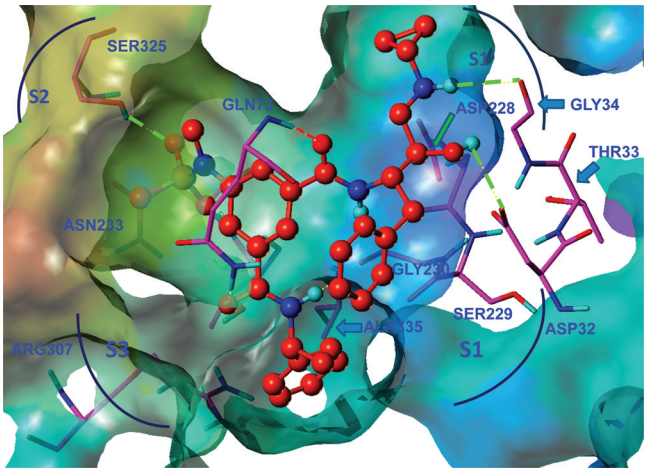

Figure 2. Top-ranked docked pose of compound **I** (ball and stick rendering, carbon atoms in red) into the BACE1 binding site based on 2B8L X-ray structure from the Protein Data Bank. The pose has a rmsd (root mean square deviation) of 0.5 Å of the pose reported for a very similar ligand in 2B8L. The protein atoms are shown in tube rendering. The four subsites S1′, S1, S2, and S3 are also marked for clarity with blue arcs.

Sybyl-X program, version 1.3 (for details, see Experimental Section).[18] Two important observations could be concluded from Figure 3. First, the methoxybenzimidazole group at the P1−P1′ position appeared not to be perfectly projected toward the S1−S1′ subpockets. Second, the NH of the imidazole ring was not properly oriented to be engaged with hydrogen bonding interaction with Asp32. At the outset of this analysis, it could be more than idle speculation at this level to suggest that such factors were responsible for lowering the affinity between these ligands and BACE1. With these results in hand, we next turned our attention toward finding proper groups that fit in the S1−S1′ subpockets. The first task in finding such potent BACE1 inhibitors was centered on proper functionalization of the imidazole ring in **III** (Figure 1).

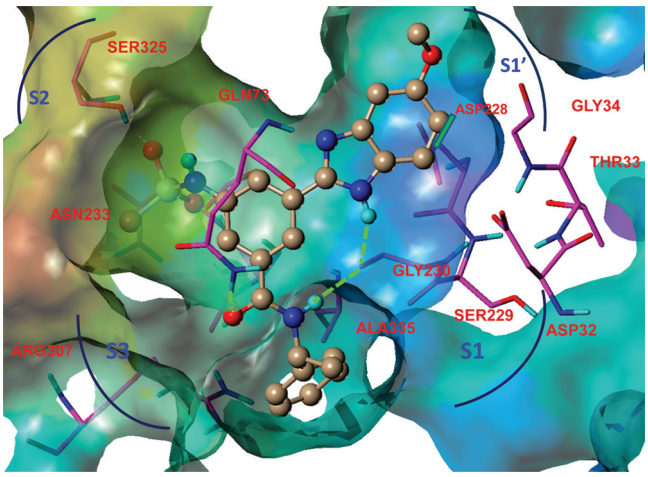

Figure 3. Top-ranked docked pose of compound **7** (ball and stick rendering, carbon atoms in gray) into the BACE1 binding site based on 2B8L X-ray structure from the Protein Data Bank. The protein atoms are shown in tube rendering. The four subsites S1′, S1, S2, and S3 are also marked for clarity with blue arcs.

Accordingly, we envisioned that an extension strategy around the imidazole ring would allow for direct projection toward the unoccupied S1−S1′ subpockets. To this end, we have introduced a phenyl group at the 4-position of the imidazole moiety leading to compounds **12**−**14** (Scheme 2). These compounds were tested for their activity profile against BACE1 and BACE2 (Table 1). As expected, compound **13** was found to be 7-fold more potent against BACE1 when compared to compound **7**. Comparable activities for compounds **12** and **13** were found in the cellular assay with an EC_{50} of 450 and 179 nM (Table 2), respectively. The selectivity index for BACE1/BACE2 was calculated to be 30. When docked using Sybyl-X 1.3 under induced-fit mode, it was found that ligand **13**, containing the more flexible methoxyphenylimidazole arm, projected directly toward S1−S1′ subpockets (Figure 4) and the

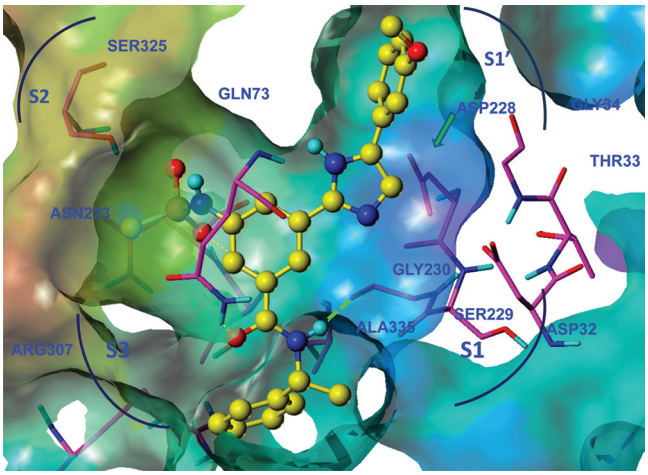

Figure 4. Top-ranked docked pose of compound **13** (green) into the BACE1 binding site.

imidazole ring and methoxy phenyl groups were properly oriented to form van der Waals (vdW) contacts with the enzyme wall as well as hydrogen bonding with Asp32 (Figure 4).

This analysis could explain the enhanced potency of compounds **12**−**14** compared to the previous series. On the

dx.doi.org/10.1021/jm201181f|J. Med. Chem. 2011, 54, 8373−8385

Table 3. SAR of BACE1 Inhibitors[a]

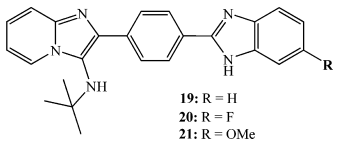

19: R = H
20: R = F
21: R = OMe

	BACE1					BACE2	
compd	IC_{50} (nM)	K_I (nM)	ELISA EC_{50} (nM)	LE (kJ/mol)	*t*PSA (Å^2)	IC_{50} (nM)	K_I (nM)
19	5511 ± 248	5312 ± 447	NA	1.04	52	5675	5509
20	2479 ± 313	2389 ± 402	NA	1.03	61.2	3725	3617
21	2241 ± 424	2160 ± 505	2405 ± 521	1.08	52.1	2895	2810

[a] IC_{50} and EC_{50} values are the mean values of at least three experiments ± SD. NA means not applicable.

other hand, the high selectivity index found for this series could be due to the difference in both the dynamic motion and the protein amino acid sequences of the "flap" loops of the BACE1 and BACE2 upon ligand engagement. This apparently may have influenced the ligand/protein contacts and impeded the ligand's affinity for the BACE2 site, thus resulting in increased selectivity.

With these promising results in hand, efforts were shifted toward further rigidification/cyclization of the prime side P3, as it was felt that this strategy was more likely to lead to the identification of druglike inhibitors of BACE1 with the potential for good oral bioavailability and CNS penetration. In this regard we calculated the PSA of compounds **6**–**8** and **12**–**14**, and these were found to be high >90 (Tables 1 and 2).[15a] It has been noted that molecules possessing a large PSA may encounter difficulty in crossing biological membranes. This inability to cross membranes may result in poor absorption or lack of blood–brain barrier (BBB) penetration. Some of the first work correlating PSA and oral absorption was published by Palm[15b] who found that drugs that were highly absorbed (>90%) had a polar surface area less than 60 Å^2 while drugs that were poorly absorbed (<10%) had a polar surface area greater than 140 Å^2.[15c]

To improve the PSA values, we next synthesized a series of fused-ring compounds, **19**–**21** (Scheme 3), which were subsequently tested for their activities against BACE1 and BACE2 (Table 3). The intended goals for the synthesis of such scaffolds were threefold: to eliminate the peptidic nature, to rigidify the system, and to decrease the PSA (Table 3). Unfortunately, this brought about a 72-fold decrease in potency toward BACE1 and a sharp decrease in the selectivity toward BACE2 when compared to the previous series. As shown in the docking pose of compound **20** (Figure 5), its functional groups were not properly oriented between S3–S1′ subpockets, resulting in low affinity toward the protein.

The decreased selectivity of these ligands could be attributed to the increased linearity of the two handles on the central phenyl ring (terephthalic acid derivative). Despite these discouraging results, it was decided to synthesize the regioisomers of compounds **19**–**21** (Scheme 4) so that the intended derivatives possessed isophthalic acid backbone similar to that present in compound **I**. The FRET assay results of these motifs against BACE1 were promising (Table 4). Compound **26** was about 12-fold more potent than its regioisomer **21** and was found to be 23-fold more selective toward BACE1 when compared to BACE2. Furthermore, the activity in the cell based assay was importantly sustained during this investigation. Compound **26** tracked well with its increased

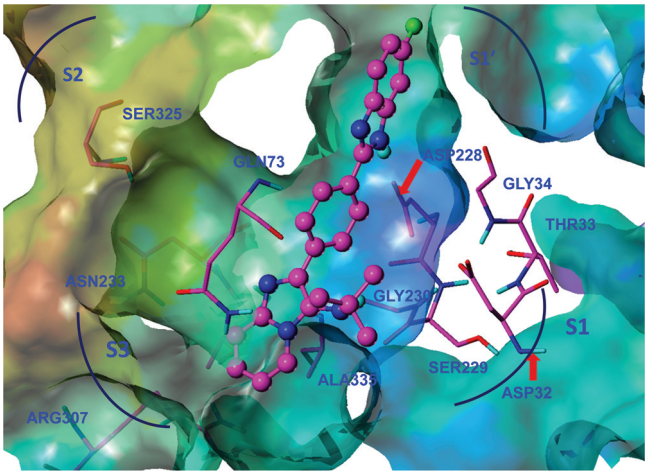

Figure 5. Top-ranked docked pose of compound **20** into the BACE1 binding site. The four subsites S1′, S1, S2, and S3 are marked for clarity with blue arcs.

molecular binding with an EC_{50} of 310 nM in the cell based ELISA assay (Table 4).

Docking analysis of compound **26** (Figure 6) indicated extensive vdW and H-bonding interactions with the protein. These included hydrogen bonding with Thr72, Gly34, Asp 32, Asp228, and Tyr14 and vdW interactions with the active site amino acid sequence. At this junction, we envisioned that the proximity of the *tert*-butyl group in **26** toward the polar parts in the active site, as could be concluded from Figure 6, may result in mutual steric clashing leading to lower affinity between this class of ligands and the enzyme active site.

Therefore, we turned our attention toward the synthesis of similar compounds devoid of such bulky arm. Thus, we carried out the synthesis of compounds **31**–**34** (Scheme 5). Their activities against BACE1 and BACE2 are shown in Table 5. Compound **34** was found to be a strongly potent inhibitor with an IC_{50} of 18 nM, which is comparable to that of compound **I** (Figure 1). Furthermore, compound **34** was found to be 204-fold more selective toward BACE1 when compared to BACE2 (IC_{50} = 3675 nM). The ligand efficiency of this compound was found to be highly promising (LE = 1.7 kJ/mol) and the PSA was 40 with Mwt of 346 Da.[15] Furthermore, compound **34** exhibited potent activity in the cell-based ELISA assay (EC_{50} = 37 nM). The enhanced potency of compound **34** could be rationalized from its docking pose (Figure 7), which is characterized by two sets of interactions: (a) hydrophobic dispersion interactions of the aromatic rings in the ligand with

dx.doi.org/10.1021/jm201181f|J. Med. Chem. 2011, 54, 8373–8385

Table 4. SAR of BACE1 Inhibitors[a]

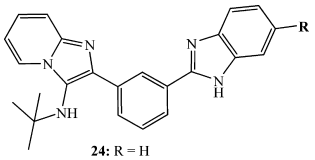

24: R = H
25: R = F
26: R = OMe

	BACE1					BACE2	
compd	IC_{50} (nM)	K_I (nM)	ELISA EC_{50} (nM)	LE (kJ/mol)	*t*PSA (Å^2)	IC_{50} (nM)	K_I (nM)
24	514 ± 110	495 ± 121	NA	1.24	52	3785	3674
25	312 ± 34	301 ± 44	930 ± 89	0.74	52	4234	4110
26	178 ± 37	253 ± 56	310 ± 29	1.21	61.3	4123	4003

[a] IC_{50} and EC_{50} values are the mean values of at least three experiments ± SD. NA means not applicable.

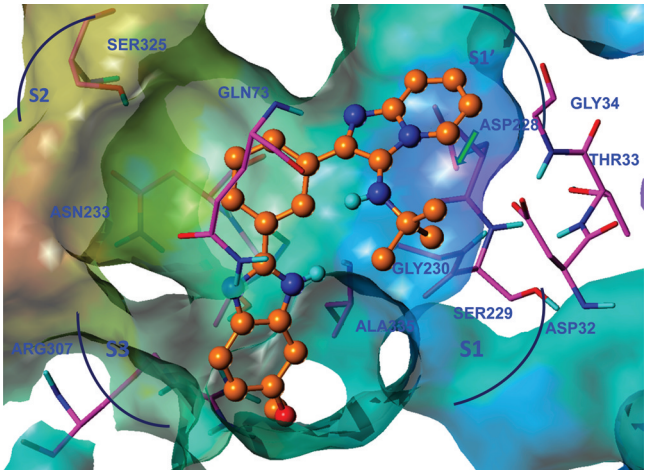

Figure 6. Top-ranked docked pose of compound **26** into the BACE1 binding site. The four subsites S1′, S1, S2, and S3 are also marked for clarity with blue arcs.

the neighboring hydrophobic side chains of amino acid residues and (b) water mediated interactions of the polar atoms in the ligand with the side chains of Asp32, Thr72, Gln328 as well as direct electrostatic interactions with the side chain of Asp228.

Removal of the *tert*-butylamine group and introduction of a fluoro- and/or methoxybenzimidazol group at the meta-position of the central phenyl nucleus (e.g., compounds **33** and **34**, Scheme 5) sharply increased the ligand potency (10-fold increase) for BACE1 and highly improved the ligand's selectivity (about 300-fold) against BACE2. Interestingly, replacement of the imidazopyridine nucleus with a fluoroimidazopyridine moiety, **32**–**34**, resulted in an additional enhancement (40-fold) of the ligand's affinity (**34** vs **31**). Furthermore, the **34**·HCl salt had appreciable solubility in distilled water (10 mg/mL; for details see Experimental Section).

CONCLUSION

In this work we have optimized the synthesis of novel, low molecular weight, and potent transition state inhibitors of BACE1. Furthermore, we have developed peptidomimetic groups to replace P1–P1′ and P3 moieties resident on compound **I**. The synthetic methodologies followed were simple, efficient, and economic. Several of the developed low molecular weight scaffolds possessed high affinity, promising ligand efficiency, and low PSA. Many of these motifs exhibited comparable cellular potency. Moreover, since the peptidic nature and the number of rotatable bonds of these motifs are low, they represent a novel class of druglike leads. On the basis of the extensive SAR analysis of the transition state inhibitors of BACE1, a pharmacophoric model (Figure 8) is proposed. In this model, a central aryl ring, disubstituted on the meta-positions with heteroaryl groups, is needed to properly orient the ligands in the active site of the protein. A hydrogen bond acceptor on the aromatic portion, resident on the heteroaryl group located on the right side of the model, enhances the affinity to BACE1 by projecting directly toward S1–S1′ subpockets. Furthermore, a fused heteroaromatic ring appendage on the left side of the proposed model projects toward S3 subpocket of the protein and is needed for improved activity. To further support this proposed model, an overlay of the most potent compounds described in this article, in the enzyme active site is depicted in Figure 9. The results described here merit further investigations and developments in our laboratories.

EXPERIMENTAL SECTION

Chemistry. Materials and General Methods. Reagents and solvents were purchased from commercial sources and were used as received. Reaction progress was monitored by thin-layer chromatography on Merck silica gel 60 F-254 with detection by UV. Silica gel 60 (Merck 40–63 μm) was used for flash column chromatography. ^{1}H NMR and ^{13}C NMR spectra were recorded with Bruker 300 and Bruker AMX-400 spectrometers using DMSO-d_6 or $CDCl_3$. Data are presented as follows: chemical shift (parts per million, ppm), multiplicity (s, singlet; d, doublet; t, triplet; q, quartet; m, multiplet; br, broad; bs, broad singlet; bd, broad doublet), coupling constant *J* (in hertz), and integration. Carbon magnetic resonance (^{13}C NMR) spectra were recorded at 75 or 125 MHz. Data for ^{13}C NMR are reported in terms of chemical shifts (ppm). High resolution mass spectra were recorded in positive ion mode by electrospray ionization (ESI) on a Bruker instrument. The samples were dissolved in acetonitrile, diluted in spray solution (methanol/water (1:1 v/v)–0.1% formic acid), and infused using a syringe pump with a flow rate of 2 mL/min. External calibration was conducted using arginine cluster in a mass range *m*/*z* 175–871. For all HRMS data, mass error was 0.00–0.50 ppm.

All compounds were determined to be >95% pure by high-performance liquid chromatography (HPLC). Purity of compounds was determined on a Phenomenex Luna C18 (2) 3 mm column, 4.6 mm i.d. × 30 mm length, with 30–75% acetonitrile/water/0.1% trifluoroacetic acid and 1.0 mL/min elution at room temperature using 210, 254, or 280 nm wavelength.

General Procedure A for the Synthesis of Compounds 6–8, 19–21, 24–26, and 31–34. To a solution of the desired carboxylic

dx.doi.org/10.1021/jm201181f|J. Med. Chem. 2011, 54, 8373–8385

Table 5. SAR of BACE1 Inhibitors[a]

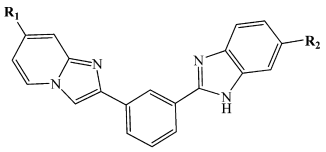

31: R1 = H, R2 = H
32: R1 = H, R2 = F
33: R1 = H, R2 = OMe
34: R1 = F, R2 = F

	BACE1					BACE2	
compd	IC_{50} (nM)	K_I (nM)	ELISA EC_{50} (nM)	LE (kJ/mol)	*t*PSA (Å^2)	IC_{50} (nM)	K_I (nM)
31	961 ± 66	926 ± 100	1550 ± 231	0.72	40	3890	3777
32	35 ± 8	34 ± 9	120 ± 21	1.38	40	3173	3081
33	26 ± 7	25 ± 8	30 ± 9	1.4	40	3321	3224
34	18 ± 2	17 ± 3	37 ± 11	1.7	40	3675	3568

[a]IC_{50} and EC_{50} values are the mean values of at least three experiments ± SD.

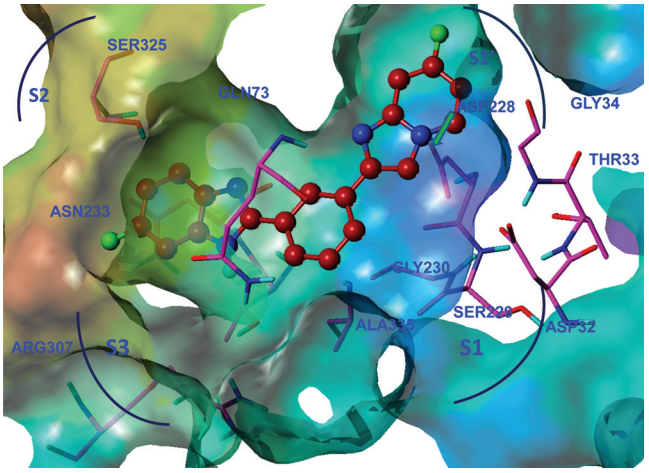

Figure 7. Top-ranked docked pose of compound **34** (ball and stick rendering, carbon atoms in magenta) into the BACE1 binding site based on 2B8L X-ray structure from the Protein Data Bank. The protein atoms are shown in tube rendering. The four subsites S1′, S1, S2, and S3 are also marked for clarity with blue arcs.

acids (**2**, **18**, **23**, **29**, or **30**) (1.0 mmol, 1 equiv) in DMF (8 mL) at 0 °C was added DIPEA (0.21 mL, 1.2 mmol, 1.2 equiv). After 10 min, TBTU (551 mg, 1.2 mmol, 1.2 equiv) was added and the resulting mixture stirred at the same temperature for 30 min. Then the desired diaminobenzene derivative (1.1 mmol, 1.1 equiv) was added. The resulting mixture was stirred at 0 °C for 6 h and then quenched with ice−water. The precipitated solid was filtered, washed with water, and dissolved in EtOAc. The organic phase was washed with a 1 N HCl aqueous solution, then with a saturated $NaHCO_3$ aqueous solution and finally H_2O, dried over $MgSO_4$, and concentrated in vacuo, which was used in the next stage without further purification. To the appropriate amide was added AcOH (30 mL), and the resulting suspension was refluxed for 6 h, cooled to room temperature, concentrated in vacuo, and diluted with crushed ice. The brown solid was filtered and washed thoroughly with water. The crude was dissolved in EtOAc, washed with a saturated $NaHCO_3$ aqueous solution and with H_2O, dried over $MgSO_4$, and concentrated in vacuo. The crude product was purified by flash chromatography on silica gel (DCM/AcOEt, 8/2 to 7/3) to give the desired benzimidazole derivative.

General Procedure B for the Synthesis of Compounds 12−14. To a solution of the carboxylic acids **2** (1.0 mmol, 1 equiv) in DMF (10 mL) at 0 °C was added DIPEA (0.21 mL, 1.2 mmol, 1.2 equiv). The resulting mixture was stirred at 0 °C for 30 min followed by dropwise addition of the appropriate α-bromoketone (1.1 mmol, 1.1 equiv) in DMF. The resulting mixture was stirred at 0 °C for 6 h, then quenched with ice−water. The precipitated solid was filtered, washed with water, and dissolved in EtOAc. The organic phase was washed with a 1 N HCl aqueous solution, saturated $NaHCO_3$ aqueous solution, H_2O, dried over $MgSO_4$, and concentrated in vacuo, which was used in the next stage without further purification. To the appropriate α-keto ester were added AcOH (25 mL) and $AcONH_4$ (924 mg, 12 mmol, 12 equiv), and the resulting suspension was refluxed for 8 h, cooled to room temperature, concentrated in vacuo, and diluted with crushed ice. The brown solid was filtered, washed thoroughly with water. The crude cake was dissolved in EtOAc, washed with a saturated $NaHCO_3$ aqueous solution, H_2O, dried over $MgSO_4$, and concentrated in vacuo. The crude product was purified by flash chromatography on silica gel (DCM/AcOEt, 8/2 to 7/3) to give compounds **12** (65%), **13** (69%), and **14** (73%).

General Procedure C for the Synthesis of Compounds 18 and 23. A mixture of the desired 2-aminopyridine (**15** or **27**) (5.1 mmol) in MeOH−DCM (2:3, 15.0 mL) and phthalaldehyde derivative (**16** or **22**, 5.0 mmol) containing 5 mol % of $Sc(OTf)_3$ was stirred for 1 h at room temperature, followed by the addition of 5.1 mmol of the *tert*-butyl isocyanide, and the mixture was stirred for another 12 h at room temperature. Then 2 mL of hexane was added, and the resulting yellowish solid was filtered, washed three times with hexane−ethyl acetate mixture (5:1, 20 mL), and triturated with ethyl acetate−hexane. The crude product was used in the next step without further purification.

General Procedure D for the Synthesis of Compounds 29 and 30. In a two-necked round-bottom flask connected with a condenser and under N_2 were introduced 2-aminopyridin derivative (**15** or **27**, 1.15 mmol), 2 methyl 3-(2-bromoacetyl)benzoate (**28**) (334 mg, 1.3 mmol), and absolute EtOH (12 mL). The reaction mixture was stirred at reflux for 2 h. After the reaction mixture had cooled down, $NaHCO_3$ (0.15 g, 1.75 mmol) was added and the mixture refluxed for another 6 h. Solvent was removed and the residue dissolved in EtOAc. The organic phase was washed thoroughly with water (three times), dried over $MgSO_4$, and filtered. The solvent was removed, and crude products were purified by washing with 5 mL of hexane. The resulting yellowish solid was filtered, washed three times with hexane−ethyl acetate mixture (5:1, 10 mL), and triturated with ethyl acetate−hexane to give crudes **29** and **30** in 67% and 61% yield, respectively. The crude products were used in the next step without further purification.

BACE1/BACE2 Enzymatic Assay. BACE1/BACE2 assays were carried out according to the manufacturer described protocol available from Invitrogen, U.S. (http://tools.invitrogen.com/content/sfs/manuals/L0724.pdf). Briefly, BACE1/BACE2 in vitro assays were carried out using fluorescence resonance energy transfer (FRET). An APP-based peptide substrate (rhodamine-EVNLDAEFK-quencher, K_M

dx.doi.org/10.1021/jm201181f|J. Med. Chem. 2011, 54, 8373−8385

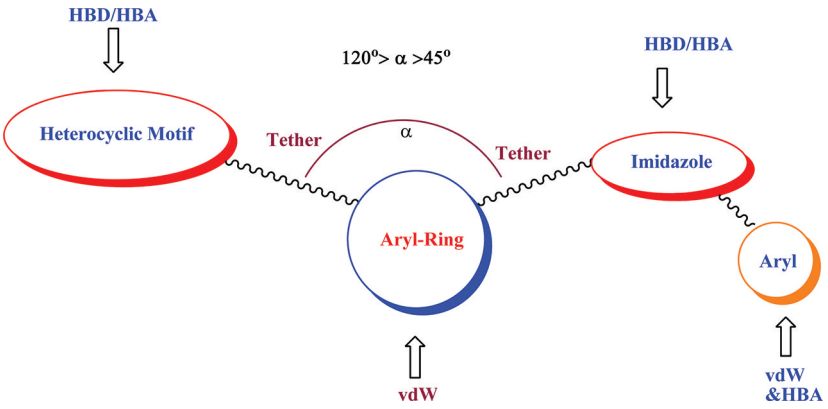

Figure 8. Proposed pharmacophoric model based on isophthalic acid BACE1 inhibitors.

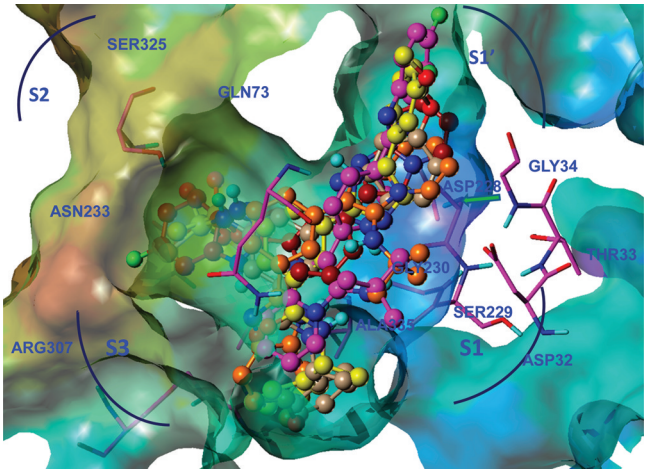

Figure 9. Overlap of top-ranked docked poses of compounds **7** (gray carbons), **13** (yellow carbons), **20** (magenta carbons), **26** (orange carbons), and **34** (red carbons) into the BACE1 binding site based on 2B8L X-ray structure from the Protein Data Bank. The overlap defines the pharmacophore of their interactions in the four subsites S1′, S1, S2, and S3 marked for clarity with blue arcs. The protein atoms are shown in tube rendering.

of 20 μM) carrying the Swedish mutation and containing a rhodamine as a fluorescence donor and a quencher acceptor at each end was used. The intact substrate is weakly fluorescent and becomes highly fluorescent upon enzymatic cleavage. The assays were conducted for both enzymes in 50 mM sodium acetate buffer, pH 4.5, in a final enzyme concentration (1 U/mL). Inhibitor (first line screening, 30, 10, 3, 1, and 0.3 μM) compounds that showed high activity at 0.3 μM were validated at low concentration, and both substrates were used at 750 nM. Inhibitor compounds were diluted from stock solutions to result in 3.3% DMSO final concentration. The mixture was incubated for 60 min at 25 °C under dark conditions and then stopped with 2.5 M sodium acetate. Fluorescence was measured with a Victor^3 1420 (Wallac) microplate reader at 545 nm excitation and 585 nm emission. The assay kit was validated by manufacturer. The obtained values are the mean values of three different experiments. IC_{50} values were calculated by plotting the obtained relative fluorescence unit per hour (RFU/h) against the logarithmic of inhibitor concentration. The measured inhibition data were analyzed in GraphPad Prism 4 for Windows (GraphPad Software Inc., La Jolla, CA, U.S.) by nonlinear regression (curve fitting). The observed inhibition constant in the presence of substrate, K_I (app), is calculated according to the following equation:

$$\frac{v_0}{v_I} = 1 + \frac{[I]}{K_I(\text{app})}$$

where v_I is the steady state rate of substrate hydrolysis in the presence of inhibitor concentration [I] and where v_0 is the uninhibited rate. From there K_I(app) can be obtained. In the case of $v_0/v_I = 2$, K_I(app) = IC_{50}. An IC_{50} is relative because it depends on substrate concentration. Therefore, an absolute K_I value can be calculated by taking into account the substrate concentration [S] and the affinity of the substrate to the enzyme, indicated by the K_M, according to the following equation:

$$K_I = \frac{K_I(\text{app})}{1 + \frac{[S]}{K_M}}$$

As an indication of the efficiency of the compounds toward binding BACE1 compared to known BACE1 inhibitors, the ligand efficiency was calculated for each compound based on the free energy equation,

$$\Delta G = -RT \ln K_I$$

and the equation of binding energy per atom (ligand efficiency, LE),

$$LE = -\Delta G/(\text{heavy atom count})$$

Cell Based Assay. Aβ42 and Aβ40 were measured in culture medium of H4 cells (human neuroglioma cell line) expressing the double Swedish mutation (K595N/M596L) of human APP (APPsw). Cells were seeded onto 24-well plates (2×10^5 cells well^{-1}) and allowed to grow for 24 h in 5% CO_2/95% air in a humidified atmosphere. Increasing concentrations of compounds were added to the cells for overnight in a final volume of 0.5 mL. *R*-Flurbiprofen was used as positive control. DMSO-d_6 (1%) was used as negative control. At the end of the incubation, an amount of 100 μL of supernatant was removed and treated with a biotinylated mouse monoclonal antibody (4G8, Signet Laboratories Inc., Dedham, MA, U.S.), specifically recognizing the 17−24 amino acid region of Aβ and two rabbit polyclonal antibodies (C-term 42 and C-term 40, BioSource International, Camarillo, CA, U.S.), specifically recognizing the C-terminus of Aβ42and Aβ40, respectively. Antigen−antibodies 5 complexes were recognized by TAG-donkey anti-rabbit IgG (Jackson Immuno Research Laboratories, Soham, U.K.). Streptavidin coated magnetic beads captured the complexes, and the signals were read by an electrochemiluminescence instrument (Origen M8 analyzer, BioVeris Corporation, Gaithersburg, MD, U.S.). The cytotoxicity potential of test compound was assessed in the same cells of the Aβ assay using the 3-[4,5-dimethylthiazol-2-yl]-2,5-diphenyltetrazolium bromide (MTT) assay. After medium removal for Aβ42 and Aβ40 determination, cells were incubated for 3 h with 500 μL of culture medium containing 0.5 mg mL^{-1} MTT at 37 °C, 5% CO_2, and saturated humidity. After removal of the medium, an amount of 25−500 μL of 100% DMSO-d_6 was added to each well. The amount of formed formazan was determined by reading the samples at 570 nm

dx.doi.org/10.1021/jm201181f|*J. Med. Chem.* 2011, 54, 8373−8385

(background, 630 nm) using a microplater reader (model 450, Bio-Rad, Hercules, CA, U.S.).

Molecular Modeling. All molecular modeling studies were carried out using the Sybyl-X program, version 1.3. The X-ray structures of the proteins in 2B8L and 3FKT were "prepared" in the presence of their respective bound ligands. These two protein−ligand complexes were chosen in light of the fact that their active sites, while being similar in size and shape, bind to their respective ligands in somewhat different modes. Interestingly, the overall three-dimensional topologies of the protein structures are very similar with minor conformational changes seen in the residues near the active site. The bound ligands were modeled to reflect their correct chemical states relevant to the binding interactions in the active site. Since the original X-ray structures do not have explicit bond orders, it is important to represent the aromaticity of rings, planarity of amides, and hybridization states of heteroatoms appropriately. The ligand preparation in Sybyl-X accounts for these states in an automated fashion. Hydrogen atoms were added on the protein atoms and on the water oxygen atoms. The orientations of water hydrogen atoms were randomly chosen. The states and orientations of the imidazole rings in histidine side chains close to the active site were adjusted to optimize interactions with the ligand and neighboring residues. In addition, the side chain amide moieties in Asn and Gln residues were also optimized for their interactions with neighboring functional groups in the bound ligand and protein residues. In each of the two cases, the protein−ligand−water complex thus obtained was subjected to a staged energy minimization which consisted of six stages: (1) minimization of hydrogen positions, (2) minimization of waters, (3) minimization of side chain atoms, (4) minimization of the entire protein structure minus the C^{α} atoms, (5) minimization of the ligand, and (6) minimization of all the atoms. In each stage, 100 cycles of energy minimizations were carried out using the Tripos force field. The main goal of this minimization is to clean up the original X-ray structure after the addition of hydrogen atoms and to orient the waters with optimal interactions toward protein residues and the bound ligand. Thus, the above procedure maintains the integrity of the experimental structures of 2B8L and 3FKT. The prepared protein−ligand−water complexes were used to generate respective protomols in Surflex-Dock[18] with the option of "Ligand". The protomols essentially represent the signatures of the active sites in docking studies with Surflex-dock. The X-ray crystallographic water molecules were retained as a segment of the protein structures during the protomol generation. Such water molecules are treated flexibly in the docking process in Surflex-Dock, with the hydrogen atoms being allowed to move while the oxygen atoms are held in place. The ligands (**7**, **13**, **20**, **26**, and **34**) were prepared using CONCORD (in the ligand preparation module of Sybyl-X) with the generation of all possible tautomeric and ionization states, where applicable. They were energy minimized using the MMFF94s force field in Sybyl-X. The prepared ligands were docked into the prepared 2B8L and 3FKT using the above generated protomols in Surflex-Dock with the GEOMX docking mode. Protein flexibility including heavy atoms and hydrogen atoms within 12 Å of the ligand poses was incorporated in the postdocking treatment of the docked poses.[18] The docked poses were examined for their hydrogen bonding interaction active site residues using the Surflex-Dock results browser in the Sybyl-X interface.

Compound 34·HCl Solubility Test. Acetonitrile (HPLC grade) was purchased from Sigma-Aldrich. Water used in the mobile phase was deionized, distilled, and filtered through a 0.45 μm Millipore filter (Sartorius, Germany) under vacuum before use. Methanol (Fluka) was HPLC grade. An Agilent HPLC system (U.S.) was used to perform the solubility test. A reversed phase high-performance liquid chromatographic method was used to test the solubility of the **34**·HCl salt in distilled water. The mobile phase was a mixture of acetonitrile and water (30:70, v/v). The flow rate was 1.0 mg/mL. The UV detector wavelength was set at 280 nm. A Waters reversed-phase C_{18} column (25 cm × 4.6 mm i.d., particle size 5 μm) was utilized as stationary phase.

Preparation of Compound 34·HCl Salt. An amount of 1 mmol of compound **34** was dissolved in 10 mL of DCM, and the mixture was cooled to 0 °C. To this solution was added dropwise 1 equiv of cold solution of concentrated HCl in 2 mL of DCM. The mixture was stirred at 0 °C for 45 min and then evaporated to dryness under high vacuum.

Calibration Curve. The calibration curve was plotted with five different concentrations of **34**·HCl salt. Five standard solutions (Table 6) were prepared in a mixture of acetonitrile/methanol, 50:50 v/v. The final concentrations of the standard solutions were 1.44, 2.50, 5.0, 10.0, and 18.0 mg/mL. The linearity was evaluated by linear regression analysis, which was calculated by the least-squares regression method. Before the solutions were injected, the column was equilibrated for at least 45 min with the mobile phase flowing through the system. Three determinations were carried out for each solution. Peak areas were recorded for all the solutions. The correlation graph was constructed by plotting peak areas obtained at the optimum wavelength of detection versus the injected amounts. A linear response was observed over the examined concentration range. Table 7 summarizes the correlation coefficient, slope, and intercept.

Table 6. Calibration Curve of Compound 34 in Acetonitrile/Methanol

concn (mg/mL)	area	slope	intercept	r^2
1.44	1739	11854	21.18	0.9995
2.5	3100			
5.0	5992			
10.0	11557			
18.0	21505			

Table 7. Compound 34·HCl Salt in Distilled Water

concn (mg/mL)	area	recovery (%)
10 (HCl in distilled water)	12073.27	99.7

Solubility Test. An accurately weighed sample of **34**·HCl salt was dissolved in distilled water to obtain a final concentration equivalent to 10 mg/mL. The solution was sonicated in a water bath for 48 h, filtered through a 0.45 μm Millipore filter, then injected into the HPLC system after running a calibration curve (Figure 10) of **34**·HCl salt dissolved into a mixture of acetonitrile/methanol, 50:50 v/v. The recovery of **34**·HCl salt was found to be 99.7% (Table 7). We found that increasing the concentration of **34** above 10 mg/mL decreased the recovery proportionally to the increasing concentration of **34**·HCl. Therefore, we concluded that the solubility is around 10 mg/mL.

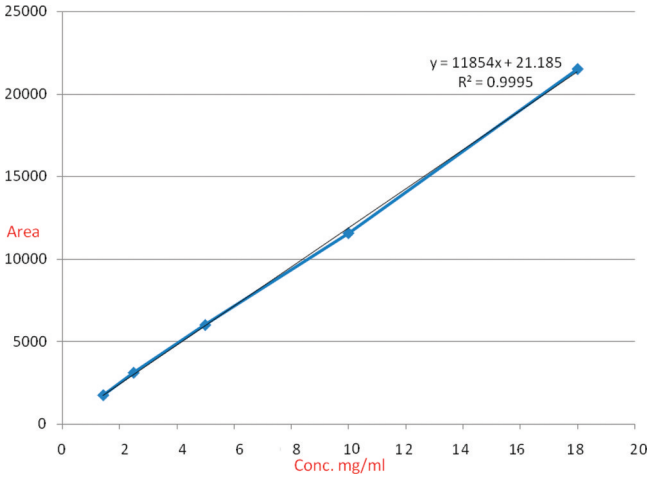

Figure 10. Calibration graph of standard solutions of **34**·HCl.

dx.doi.org/10.1021/jm201181f|J. Med. Chem. 2011, 54, 8373−8385

(*S*)-3-(Methylsulfonamido)-5-(1-phenylethylcarbamoyl)-benzoic Acid (2). ^{1}H NMR (DMSO-d_6): δ 9.14 (1H, d, J = 8.1Hs), 8.39 (1H, d, J = 1.5Hs), 8.11 (1H, dd, J = 1.8, 3.6 Hz), 8.06 (1H, dd, J = 1.8, 3.3 Hz), 7.41−7.22 (5H, m), 5.18 (1H, t, J = 7.2 Hz), 3.00 (3H, s), 2.49 (3H,s), 1.49 (3H, d, J = 7.2 Hz). HRMS: m/z [M + Na] calcd for $C_{17}H_{18}N_2O_5SNa$, 385.3922 g/mol; found, 385.3795.

(*S*)-3-(1*H*-Benzo[*d*]imidazol-2-yl)-5-(*N*-methylmethylsulfonamido)-*N*-(1-phenylethyl)benzamide (6). The synthetic procedure was the same as general procedure A. Yield 68%. ^{1}H NMR ($CDCl_3$): δ 8.29 (1H, t, J = 1.8 Hz), 7.60 (2H, m), 7.45 (1H, bs), 7.36 (1H, bs), 7.21 (2H, dd, J = 3.0, 6.6 Hz), 7.17−6.97 (6H, m), 6.38 (1H, bs), 5.33 (1H, dd, J = 8.3, 13.9 Hz), 3.14 (3H, S), 2.76 (3H, s), 1.51 (3H, d, J = 6.8). ^{13}C NMR ($CDCl_3$): δ 167.1, 155.9, 143.0, 139.7, 139.2, 136.9, 132.5, 129.1, 129.0, 128.5, 123.6, 122.1, 120.5, 118.1, 111.4, 52.8, 41.1, 34.4, 14.2. HRMS: m/z [M + Na] calcd for $C_{24}H_{24}N_4O_3SNa$, 471.5299 g/mol; found, 471.1449.

(*S*)-3-(5-Methoxy-1*H*-benzo[*d*]imidazol-2-yl)-5-(*N*-methylmethylsulfonamido)-*N*-(1-phenylethyl)benzamide (7). The synthetic procedure was the same as general procedure A. Yield 72%. ^{1}H NMR ($CDCl_3$): δ 8.30 (1H, bs), 8.1 (1H, bs), 7.74 (1H, bs), 7.41 (1H, bd, J = 8.7 Hz), 7.27−7.15 (6H, m), (1H, bs), 6.85 (1H, dd, J = 2.1, 9.0 Hz), 5.19 (1H, t, J = 7.2 Hz), 3.77 (3H, s), 3.15 (3H, s), 2.70 (3H,s), 1.48 (3H, d, J = 6.9 Hz). ^{13}C NMR ($CDCl_3$): δ 169.7, 160.1, 158.3, 146.1, 145.1, 141.2, 138.5, 133.4, 131.2, 129.7, 128.8, 128.2, 123.4, 121.1, 120.3, 114.2, 111.3, 99.1, 55.3, 48.2, 38.2, 32.3, 14.3. HRMS: m/z [M + Na] calcd for $C_{25}H_{26}N_4O_4SNa$, 501.5560 g/mol; found, 501.1554.

(*S*)-3-(5-Fluoro-1*H*-benzo[*d*]imidazol-2-yl)-5-(*N*-methylmethylsulfonamido)-*N*-(1-phenylethyl)benzamide (8). The synthetic procedure was the same as general procedure A. Yield 62%. ^{1}H NMR ($CDCl_3$): δ 8.28, (1H, dd, J = 1.8, 4.2 Hz), 8.25 (1H, d, J = 8.7 Hz), 7.50 (1H, dd, J = 2.7, 5.4 Hz), 7.47 (1H, d, J = 4.5 Hz), 7.37 (1H, d, J = 4.8 Hz), 7.14 (3H, m), 6.97 (3H, m), 6.37 (1H, bs), 5.34 (1H, dd, J = 8.4, 14.4 Hz), 3.15 (3H, s), 2.72 (3H, s), 1.46 (3H, d, J = 6.9 Hz). ^{13}C NMR ($CDCl_3$): δ 167.1, 156.8, 155.9, 153.3, 143.8, 143.7, 143.1, 139.7, 136.7, 131.4, 128.4, 128.1, 127.6, 121.2, 119.6, 116.2, 116.1, 114.9, 114.6, 112.2, 111.8, 110.2, 49.7, 38.4, 31.9, 14.3. HRMS: m/z [M + Na] calcd for $C_{24}H_{23}FN_4O_3SNa$, 489.5203 g/mol; found, 489.1360.

(*S*)-3-(*N*-Methylmethylsulfonamido)-5-(5-phenyl-1*H*-imidazol-2-yl)-*N*-(1-phenylethyl)benzamide (12). The synthetic procedure was the same as general procedure B. Yield 65%. ^{1}H NMR ($CDCl_3$): δ 8.0 (1H, bs), 7.84 (1H, bs), 7.68 (2H, bd, J = 7.2H), 7.50 (2H, bs), 7.35−7.19 (10H, m), 5.13 (1H, t, J = 7.2 Hz), 3.04 (3H, s), 2.60 (3H, s), 1.48 (3H, d, J = 6.9 Hz). ^{13}C NMR ($CDCl_3$): δ 171.1, 166.0, 145.4, 142.9, 141.8, 135.9, 131.5, 128.7, 128.5, 127.3, 127.1, 126.2, 126.1, 125.7, 124.9, 124.2, 122.3, 60.3, 49.9, 37.5, 35.4, 21.6, 20.9, 14.1. HRMS: m/z [M + Na] calcd for $C_{26}H_{26}N_4O_3SNa$, 497.5673 g/mol; found, 497.1621.

(*S*)-3-(5-(3-Methoxyphenyl)-1*H*-imidazol-2-yl)-5-(*N*-methylmethylsulfonamido)-*N*-(1-phenylethyl)benzamide (13). The synthetic procedure was the same as general procedure B. Yield 69%. ^{1}H NMR ($CDCl_3$): δ 8.37 (1H, d, J = 2.1 Hz), 8.00 (1H, d, J = 9.97), 7.52 (1H, dd, J = 8.4 Hz), 7.45 (2H, d, J = 4.8 Hz), 7.43 (1H, s), 7.15 (2H, dd, J = 2.7, 4.5 Hz), 7.05−6.92 (5H, m), 5.34 (1H, t, J = 8.4 Hz), 3.91 (3H, s), 2.71 (3H,s), 1.50 (3H, d, J = 6.9 Hz). ^{13}C NMR ($CDCl_3$): δ 170.0, 162.1, 151.2, 145.1, 141.3, 139.7, 138.2, 133.6, 130.5, 129.6, 129.6, 129.1, 128.5, 125.4, 123.3, 123.1, 121.9, 120.2, 119.8, 112.1, 110.5, 53.4, 50.1, 39.3, 32.2, 14.1. HRMS: m/z [M + Na] calcd for $C_{27}H_{28}N_4O_4SNa$, 527.5934 g/mol; found, 527.5832.

(*S*)-3-(5-(3-Fluorophenyl)-1*H*-imidazol-2-yl)-5-(*N*-methylmethylsulfonamido)-*N*-(1-phenylethyl)benzamide (14). The synthetic procedure was the same as general procedure B. Yield 73%. ^{1}H NMR ($CDCl_3$): δ 8.13, (1H,bs), 7.94 (1H,bs), 7.63 (3H, m), 7.32−7.23 (6H, m), 7.09 (1H, bs), 7.00 (2H, t, J = 8.7 Hz), 5.18 (1H, t, J = 7.21 Hz), 3.16 (3H, s), 2.73 (3H, s), 1.51 (3H, d, J = 6.9 Hz). ^{13}C NMR ($CDCl_3$): δ 171.1, 166.0, 163.7, 160.3, 145.4, 142.8, 141.9, 135.9, 131.6, 128.6, 127.3, 126.5, 126.4, 126.0, 124.2, 123.4, 115.6, 115.1, 60.3, 49.9, 37.7, 35.5, 14.1. HRMS: m/z [M + Na] calcd for $C_{26}H_{25}FN_4O_3SNa$, 515.5578 g/mol; found, 515.1522.

4-(3-(*tert*-Butylamino)imidazo[1,2-*a*]pyridin-2-yl)benzoic Acid (18). The synthetic procedure was the same as general procedure C. Yield 73%. The synthetic procedure was the same as general procedure A. Yield 67%. ^{1}H NMR (DMSO-d_6): δ 8.39 (1H, d, J = 6.9 Hz), 8.26 (2H, m), 7.99 (2H, bs), 7.44 (1H, bs), 7.20 (1H, d, J = 6.9 Hz), 6.88 (1H, t, J = 6.9 Hz), 4.65 (1H, bs), 0.98 (9 H, s). HRMS: m/z [M + Na] calcd for $C_{18}H_{19}N_3O_2Na$, 332.3538 g/mol; found, 332.3419.

2-(4-(1*H*-Benzo[*d*]imidazol-2-yl)phenyl)-*N*-*tert*-butylimidazo-[1,2-*a*]pyridin-3-amine (19). The synthetic procedure was the same as general procedure A. Yield 73%. ^{1}H NMR ($CDCl_3$): δ 6.04 (1H, d, J = 6.9 Hz), 5.94 (2H, d, J = 8.4 Hz), 5.82 (2H, d, J = 8.4 Hz), 5.41 (1H, dd, J = 3.3, 6.0 Hz), 5.28 (1H, d, J = 9.0 Hz), 5.01 (4H, m), 4.61 (1H, t, J = 6.6 Hz), 1.20 (9H, s). ^{13}C NMR ($CDCl_3$): δ 152.1, 147.8, 144.8, 139.9, 137.9, 133.9, 132.2, 132.1, 124.7, 124.4, 122.5, 121.0, 120.2, 119.6, 118.5, 112.3, 110.7, 107.7, 51.8, 26.0. HRMS: m/z [M + H] calcd for $C_{24}H_{24}N_5$, 382.4830 g/mol; found, 382.2047.

***N*-*tert*-Butyl-2-(4-(6-fluoro-1*H*-benzo[*d*]imidazol-2-yl)-phenyl)imidazo[1,2-*a*]pyridin-3-amine (20).** The synthetic procedure was the same as general procedure A. Yield 65%. ^{1}H NMR ($CDCl_3$): δ 8.24 (1H, d, J = 6.9 Hz), 8.0 (2H, d, J = 8.4 Hz), 7.81 (2H, d, J = 8.4 Hz), 7.5 (1H, d, J = 9.3 Hz), 7.47 (1H, m), 7.16 (2H, m), 6.91 (1H, t, J = 1.8 Hz), 6.82 (1H, t, J = 6.9 Hz), 0.97 (9H, s). ^{13}C NMR ($CDCl_3$): δ 161.0, 157.8, 153.2, 144.8, 144.4, 141.8, 138.4, 136.0, 128.9, 128.5, 126.8, 125.0, 124.1, 123.6, 116.1, 111.4, 110.8, 110.4, 56.4, 30.1. HRMS: m/z [M + Na] calcd for $C_{24}H_{22}FN_5Na$, 422.4553 g/mol; found, 422.1749.

***N*-*tert*-Butyl-2-(4-(6-methoxy-1*H*-benzo[*d*]imidazol-2-yl)-phenyl)imidazo[1,2-*a*]pyridin-3-amine (21).** The synthetic procedure was the same as general procedure A. Yield 69%. ^{1}H NMR ($CDCl_3$): δ 8.77 (1H, d, J = 7.8 Hz), 8.14 (1H, d, J = 8.4 Hz), 7.87 (3H, m), 7.48 (1H, d, J = 8.4 Hz), 7.16 93H, m), 6.85 (1H, t, J = 6.6 Hz), 3.86 (3H, s), 1.20 (9H, s). ^{13}C NMR ($CDCl_3$): δ 155.2, 152.1, 144.8, 142.3, 133.3, 131.5, 128.6, 127.9, 124.2, 123.7, 118.7, 117.1, 113.2, 112.0, 105.3, 98.3, 55.3, 54.6, 31.1. HRMS: m/z [M + Na] calcd for $C_{25}H_{25}N_5ONa$, 434.4910 g/mol; found, 434.1947.

3-(3-(*tert*-Butylamino)imidazo[1,2-*a*]pyridin-2-yl)benzoic Acid (23). The synthetic procedure was the same as general procedure C. Yield 71%. ^{1}H NMR (DMSO-d_6): δ 8.84 (1H, bs), 8.44 (1H, bs), 8.42 (1H, bs), 7.84 (1H, bs), 7.51 (1H, bs), 7.48 (1H, bs), 7.24 (1H, d, J = 8.1 Hz), 6.93 (1H, t, J = 6.9 H), 4.71 (1H, bs), 1.01 (9H, s). HRMS: m/z [M + Na] calcd for $C_{18}H_{19}N_3O_2Na$, 332.3538 g/mol; found, 332.3431.

2-(3-(1*H*-Benzo[*d*]imidazol-2-yl)phenyl)-*N*-*tert*-butylimidazo-[1,2-*a*]pyridin-3-amine (24). The synthetic procedure was the same as general procedure A. Yield 65%. ^{1}H NMR ($CDCl_3$): δ 8.77 (1H, d, J = 7.8 Hz), 8.51 (1H, bs), 8.35 (1H, t, J = 8.1 Hz), 8.20 (1H. d, J = 9.0 Hz), 7.85 (2H, m), 7.59 (2H, m), 7.23 (3H, m), 6.84 (1H, t, J = 8.1 Hz), 1.2 (9H, s). ^{13}C NMR ($CDCl_3$): δ 153.2, 144.8, 138.8, 137.1, 132.0, 130.0, 129.1, 128.7, 127.9, 125.0, 124.0, 123.7, 123.5, 118.7, 116.1, 112.0, 105.2, 54.6, 31.1. HRMS: m/z [M + Na] calcd for $C_{24}H_{23}N_5Na$, 404.4649 g/mol; found, 404.1840.

***N*-*tert*-Butyl-2-(3-(6-fluoro-1*H*-benzo[*d*]imidazol-2-yl)-phenyl)imidazo[1,2-*a*]pyridin-3-amine (25).** The synthetic procedure was the same as general procedure A. Yield 68%. ^{1}H NMR ($CDCl_3$): δ 6.61 (1H, bs), 6.49 (1H, d, J = 6.7 Hz), 6.24 (1H, d, J = 7.8 Hz), 6.10 (1H, d, J = 7.8 Hz), 5.69 (3H, m), 5.53 (1H,d, J = 6.9 Hz), 5.41 (1H, t = 7.8 Hz), 5.20 (1H, dt, J = 2.4, 9.0, 11.4 Hz), 5.03 (1 H, t, J = 6.6 Hz), 1.00 (9H, s). ^{13}C NMR ($CDCl_3$): δ 156.8, 153.3, 153.2, 144, 143.4,143.3, 137.1, 133.0, 132.9, 132.1, 130.1, 129.5, 129.0, 128.2, 125.1, 124.1, 123.9, 119.1, 117.0, 116.4, 115.3, 114.9, 113.1, 111.6. HRMS: m/z [M + Na] calcd for $C_{24}H_{22}FN_5Na$, 422.4553 g/mol; found, 422.1741.

***N*-*tert*-Butyl-2-(3-(6-methoxy-1*H*-benzo[*d*]imidazol-2-yl)-phenyl)imidazo[1,2-*a*]pyridin-3-amine (26).** The synthetic procedure was the same as general procedure A. Yield 58%. ^{1}H NMR ($CDCl_3$): δ 8.11 (1H, bs), 8.00 (1H, d, J = 6.9 Hs), 7.68 (1H, d, J = 7.8 Hz), 7.59 (1H, d, J = 7.8 Hz), 7.23−7.09 (3H, m), 6.85 (1H, t, J = 8.1 Hz), 6.76 (1H, d, J = 1.8 Hz), 6.56 (1H, dd, J = 2.1, 8.7 Hz), 6.5 (1H, d, J = 6.6 Hz), 3.52 (3H,s), 1.12 (9H, s). ^{13}C NMR ($CDCl_3$): δ 156.3, 151.31, 141.6, 137.9, 135.1, 129.4, 129.3, 128.8, 125.8, 125.1,

dx.doi.org/10.1021/jm201181f|J. Med. Chem. 2011, 54, 8373−8385

124.9, 124.3, 124.0, 115.8, 113.1, 111.5, 55.9, 55.3, 29.5. HRMS: *m*/*z* [M + Na] calcd for $C_{25}H_{25}N_5ONa$, 434.4910 g/mol; found, 434.1954.

2-(3-(Imidazo[1,2-*a*]pyridin-2-yl)phenyl)-1*H*-benzo[*d*]-imidazole (31). The synthetic procedure was the same as general procedure A. Yield 66%. ^{1}H NMR ($CDCl_3$): δ 8.59 (1H, d, J = 8.1 Hz), 8.38 (2H, m), 7.89 (1H, bs), 7.83 (1H, m), 7.59 (6H, m), 7.34 (1H, m), 7.23 (2H, dd, J = 3.3, 6.3 H), 7.00 (2H, t, J = 1.2 Hz). ^{13}C NMR ($CDCl_3$): δ 153.2, 151.0, 147.5, 138.8, 133.9, 130.6, 128.7, 128.4, 126.6, 126.2, 125.7, 123.9, 123.5, 116.1, 115.0, 112.4, 103.0. HRMS: *m*/*z* [M + Na] calcd for $C_{20}H_{14}N_4Na$, 333.3435 g/mol; found, 333.2437.

6-Fluoro-2-(3-(imidazo[1,2-*a*]pyridin-2-yl)phenyl)-1*H*-benzo-[*d*]imidazole (32). The synthetic procedure was the same as general procedure A. Yield 61%. ^{1}H NMR ($CDCl_3$): δ 9.06 (1H, bs), 8.59 (1H, d, J = 8.1 Hz), 8.37 (2H, m), 8.25 (1H, d, J = 9.0 Hz), 7.93 (1H, bs), 7.82 (1H, dd, J = 1.2, 3.0 Hz), 7.64 (1H, bd, J = 8.4 Hz), 7.51 (1H, dd, J = 2.7, 5.4 Hz), 7.35 (1H, t, J = 6.6 Hz), 7.14 (1H, t, J = 3.9 Hz), 6.97 (1H,t, J = 5.4 Hz). ^{13}C NMR ($CDCl_3$): δ 156.8,153.4, 153.2, 151.0, 147.5, 143.5, 143.1, 133.9, 133.0, 132.7, 129.8, 129.0, 128.6, 127.0, 126.8, 126.1, 123.8, 117.1, 116.7, 115.3, 115.1, 114.7, 113.0, 129.6, 111.8, 103.1. HRMS: *m*/*z* [M + Na] calcd for $C_{20}H_{13}FN_4Na$, 351.3340 g/mol; found, 351.3253.

2-(3-(Imidazo[1,2-*a*]pyridin-2-yl)phenyl)-6-methoxy-1*H*-benzo[*d*]imidazole (33). The synthetic procedure was the same as general procedure A. Yield 69%. ^{1}H NMR ($CDCl_3$): δ 9.06 (1H, bs), 8.6 (1H,d, J = 8.1 Hz), 8.40 (2H,m), 7.93 (1H, bs), 7.81 (1H, dd, J = 1.5, 4.7 Hz), 7.75 (1H, bd, J = 8.3 Hz), 7.48 (1H, bd, J = 8.4 Hz), 7.34 (1H, t, J = 8.7 Hz), 7.15 (1H, dd, J = 2.7, 8.4 Hz), 7.10 (1H, bd, J = 3.0 Hz), 7.0 (1H, t, J = 6.6 Hz), 3.86 (3H,s). ^{13}C NMR ($CDCl_3$): δ 155.2, 153.2, 151.0, 147.5, 141.1, 133.8, 130.5, 130.3, 128.7, 128.4, 126.6, 126.2, 125.7, 123.9, 117.1, 115.0, 113.2, 112.4, 103.0, 98.3, 55.3. HRMS: *m*/*z* [M + Na] calcd for $C_{21}H_{16}N_4ONa$, 363.3696 g/mol; found, 363.3479.

6-Fluoro-2-(3-(7-fluoroimidazo[1,2-*a*]pyridin-2-yl)phenyl)-1*H*-benzo[*d*]imidazole (34). The synthetic procedure was the same as general procedure A. Yield 63%. ^{1}H NMR ($CDCl_3$): δ 9.14 (1H,s), 8.29 (2H,m), 8.24 (2H,m), 7.93 (1H,bs), 7.82 (2H,m), 7.51 (1H, dd, J = 2.7,5.4 Hz), 7.26 (1H, bd, J = 1.0 Hz), 7.13 (1H, dd, J = 2.4,5.1 Hz), 7.10 (1H, dd, J = 2.4, 5.1 Hz). ^{13}C NMR ($CDCl_3$): δ 156.8, 153.4, 153.2, 151.0, 147.6, 147.5, 143.4, 143.3, 133.9, 133.1, 133.0, 129.6, 128.7, 128.4, 126.5, 126.4, 125.7, 123.9, 116.2, 116.1, 114.9, 114.6, 112.2, 111.8, 105.0, 104.6, 103.0, 98.1, 97.9. HRMS: *m*/*z* [M + Na] calcd for $C_{20}H_{12}F_2N_4Na$, 369.3244 g/mol; found, 369.3122.

■ ASSOCIATED CONTENT

Ⓢ Supporting Information

Experimental procedures for the synthesis of **6**−**34**, in vitro assays and protocols for the determination of K_I, and dose response curves. This material is available free of charge via the Internet at http://pubs.acs.org.

■ AUTHOR INFORMATION

Corresponding Author

*Phone: (971) 50 1732950. Fax: +971 6 5585812. E-mail: taltal@sharjah.ac.ae.

■ ACKNOWLEDGMENTS

The authors are grateful to the College of Graduate Studies and Research (University of Sharjah, UAE) for partially funding this research project. Dr. Thomas Nittoli and Dr. Sana Enayeh are greatly acknowledged for their valuable discussions and proofreading.

■ ABBREVIATIONS USED

AD, Alzheimer's disease; APP, amyloid precursor protein; BACE1, β-site amyloid precursor protein cleaving enzyme 1; HPLC, high performance liquid chromatography; SAR, structure−activity relationship; PSA, polar surface area; LC−MS, liquid chromatography−mass spectrometry; DCM, dichloromethane; DMF, *N*,*N*-dimethylformamide; DIPEA, *N*,*N*-diisopropylethylamine; HE, hydroxyethylene; FRET, fluorescence resonance energy transfer; FRU/h, relative fluorence unit per hour; LE, ligand efficiency; ELISA, enzyme-linked immunosorbent assay; HRMS, high resolution mass spectrometry

■ REFERENCES

(1) Winblad, B.; Wimo, A. Pharmacoeconomics in Alzheimer's disease. *Neurodegener. Dis.* **2007**, *4*, 5−11.

(2) Alzheimer's Association. 2009 Alzheimer's disease facts and figures. *Alzheimer's Dementia* **2009**, *5*, 234−270.

(3) (a) Selkoe, D. J.; Schenk, D. Alzheimer's disease: molecular understanding predicts amyloid-based therapeutics. *Annu. Rev. Pharmacol. Toxicol.* **2003**, *43*, 545−584. (b) Hardy, J.; Selkoe, D. J. The amyloid hypothesis of Alzheimer's disease: progress and problems on the road to therapeutics. *Science* **2002**, *297*, 353−356.

(4) Citron, M. Strategies for disease modification in Alzheimer's disease. *Nat. Rev. Neurosci.* **2004**, *5*, 677−685.

(5) (a) Bu, G. Apolipoprotein E and its receptors in Alzheimer's disease: pathways, pathogenesis and therapy. *Nat. Rev. Neurosci.* **2009**, *10*, 333−344. (b) Walsh, D. M.; Selkoe, D. J. Aβ oligomers—a decade of discovery. *J. Neurochem.* **2007**, *101*, 1172−1184. (c) Haass, C. Amyloid peptide is produced by cultured cells during normal metabolism. *Nature* **1992**, *359*, 322−325.

(6) (a) Leung, D.; Abbenante, G.; Fairlie, D. P. Protease inhibitors: current status and future prospects. *J. Med. Chem.* **2000**, *43*, 305−341. (b) Durham, T. B.; Shepherd, T. A. Progress toward the discovery and development of efficacious BACE inhibitors. *Curr. Opin. Drug Discovery Dev.* **2006**, *9*, 776−791.

(7) Citron, M. β-Secretase inhibition for the treatment of Alzheimer's disease—promise and challenge. *Trends Pharmacol. Sci.* **2004**, *25*, 59−112.

(8) (a) Gerlai, R. Gene-targeting studies of mammalian behavior: Is it the mutation or the background genotype? *Trends Neurosci.* **1996**, *19*, 177−181. (b) Hu, X. BACE1 modulates myelination in the central and peripheral nervous system. *Nat. Neurosci.* **2006**, *9*, 1520−1525. (c) Sankaranarayanan, S. In vivo β-secretase 1 inhibition leads to brain A β lowering and increased β-secretase processing of amyloid precursor protein without effect on neuregulin-1. *J. Pharmacol. Exp. Ther.* **2008**, *324*, 957−969. (d) Hu, X. Genetic deletion of *BACE1* in mice affects remyelination of sciatic nerves. *FASEB J.* **2008**, *22*, 2970−2980. (e) Harrison, S. M. BACE1 β-secretase transgenic and knockout mice: identification of neurochemical deficits and behavioral changes. *Mol. Cell. Neurosci.* **2003**, *24*, 646−655.

(9) CoMentis. Press Release Jul 28, 2008. CoMentis and Astellas To Present Alzheimer's Disease Research at International Conference on Alzheimer's Disease (ICAD). http://www.athenagen.com/index.php?/athenagen/press_releases/52/ (2008).

(10) (a) Durham, T. B.; Shepherd, T. A. Progress toward the discovery and development of efficacious BACE inhibitors. *Curr. Opin. Drug Discovery Dev.* **2006**, *9*, 776−791. (b) Iserloh, U.; Wu, Y.; Cumming, J. N.; Pan, J.; Wang, L. Y.; Stamford, A. W.; Kennedy, M. E.; Kuvelkar, R.; Chen, X.; Parker, E. M.; Strickland, C.; Voigt, J. Potent pyrrolidine- and piperidine-based BACE-1 inhibitors. *Bioorg. Med. Chem. Lett.* **2008**, *18*, 414−417. (c) Cumming, J.; Babu, S.; Huang, Y.; Carrol, C.; Chen, X.; Favreau, L.; Greenlee, W.; Guo, T.; Kennedy, M.; Kuvelkar, R.; Le, T.; Li, G.; McHugh, N.; Orth, P.; Ozgur, L.; Parker, E.; Saionz, K.; Stamford, A.; Strickland, C.; Tadesse, D.; Voigt, J.; Zhang, L.; Zhang, Q. Piperazine sulfonamide BACE1 inhibitors: design, synthesis, and in vivo characterization. *Bioorg. Med. Chem. Lett.* **2010**, *20*, 2837−2842. (d) Iserloh, U.; Pan, J.; Stamford, A. W.; Kennedy, M. E.; Zhang, Q.; Zhang, L.; Parker, E. M.; Mchugh, N. A.; Favreau, L.; Strickland, C.; Voigt, J. Discovery of an orally efficacious 4-phenoxypyrrolidine-based BACE-1 inhibitor. *Bioorg. Med. Chem. Lett.* **2008**, *18*, 418−422. (e) Clarke, B.; Demont, E.; Dingwall, C.; Dunsdon, R.; Faller, A.; Hawkins, J.; Hussain, I.; MacPherson, D.;

Maile, G.; Matico, R.; Milner, P.; Mosley, J.; Naylor, A.; O'Brien, A.; Redshaw, S.; Riddell, D.; Rowland, P.; Soleil, V.; Smith, K.; Stanway, S. BACE-1 inhibitors part 2: identification of hydroxy ethylamines (HEAs) with reduced peptidic character. *Bioorg. Med. Chem. Lett.* **2008**, *18*, 1017−1022. (f) Malamas, M. S.; Erdei, J.; Gunawan, I.; Barnes, K.; Johnson, M.; Hui, Y.; Turner, J.; Hu, Y.; Wagner, E.; Fan, K.; Olland, A.; Bard, J.; Robichau, A. J. Aminoimidazoles as potent and elective human β-secretase (BACE1) inhibitors. *J. Med. Chem.* **2009**, *52*, 6314−6323. (g) Malamas, M. S.; Erdei, J.; Gunawan, I.; Barnes, K.; Johnson, M.; Hui, Y.; Turner, J.; Hu, Y.; Wagner, E.; Fan, K.; Olland, A.; Bard, J.; Robichau, A. J. Design and synthesis of 5,5-disubstituted aminohydantoins as potent and selective human β-secretase (BACE1) inhibitors. *J. Med. Chem.* **2010**, *53*, 1146−1158.

(11) (a) Congreve, M.; Aharony, D.; Albert, J.; Callaghan, O.; Campbell, J.; Carr, R. A. E.; Chessari, G.; Cowan, S.; Edwards, P. D.; Frederickson, M.; McMenamin, R.; Murray, C. W.; Patel, S.; Wallis, N. Application of fragment screening by X-ray crystallography to the discovery of aminopyridines as inhibitors of beta-secretase. *J. Med. Chem.* **2007**, *50*, 1124−1132. (b) Zhu, Z.; Sun, Z.; Ye, Y.; Voigt, J.; Strickland, C.; Smith, E.; Cumming, J.; Wang, L.; Wong, J.; Wang, Y.; Wyss, D.; Chen, X.; Kuvelkar, R.; Kennedy, M.; Favreau, L.; Parker, E.; McKittrick, B.; Stamford, A.; Czarniecki, M.; Greenlee, W.; Hunter, J. Discovery of cyclic acylguanidines as highly potent and selective β-site amyloid cleaving enzyme (BACE) inhibitors: Part I—Inhibitor design and validation. *J. Med. Chem.* **2010**, *53*, 951−965.

(12) (a) Charrier, N.; Clarke, B.; Cutler, L.; Demont, E.; Dingwall, C.; Dunsdon, R.; Hawkins, J.; Howes, C.; Hubbard, J.; Hussain, I.; Maile, G.; Matico, R.; Mosley, J.; Naylor, A.; O'Brien, A.; Redshaw, S.; Rowland, P.; Soleil, V.; Smith, K.; Sweitzer, S.; Theobald, P.; Vesey, D.; Walter, D.; Wayne, G. Second generation of BACE-1 inhibitors. Part 1: The need for improved pharmacokinetics. *Bioorg. Med. Chem. Lett.* **2009**, *19*, 3664−3668. (b) Charrier, N.; Clarke, B.; Demont, E.; Dingwall, C.; Dunsdon, R.; Hawkins, J.; Hubbard, J.; Hussain, I.; Maile, G.; Matico, R.; Mosley, J.; Naylor, A.; O'Brien, A.; Redshaw, S.; Rowland, P.; Soleil, V.; Smith, K.; Sweitzer, S.; Theobald, P.; Vesey, D.; Walter, D.; Wayne, G. Second generation of BACE-1 inhibitors part 2: optimisation of the non-prime side substituent. *Bioorg. Med. Chem. Lett.* **2009**, *19*, 3669−3673. (c) Charrier, N.; Clarke, B.; Cutler, L.; Demont, E.; Dingwall, C.; Dunsdon, R.; Hawkins, J.; Howes, C.; Hubbard, J.; Hussain, I.; Maile, G.; Matico, R.; Mosley, J.; Naylor, A.; O'Brien, A.; Redshaw, S.; Rowland, P.; Soleil, V.; Smith, K.; Sweitzer, S.; Theobald, P.; Vesey, D.; Walter, D.; Wayne, G. Second generation of BACE-1 inhibitors part 3: towards non hydroxyethylamine transition state mimetics. *Bioorg. Med. Chem. Lett.* **2009**, *19*, 3674−3678. (d) Barrow, J.; Rittle, K.; Ngo, P.; Selnick, H.; Graham, S.; Pitzenberger, S.; McGaughey, G.; Colussi, D.; Lai, M.-T.; Huang, Q.; Tugusheva, K.; Espeseth, A.; Simon, A.; Munshi, S.; Vacca, J. Design and synthesis of 2,3,5-substituted imidazolidin-4-one inhibitors of BACE-1. *ChemMedChem* **2007**, *2*, 995−999.

(13) Dominguez, D.; Tournoy, J.; Hartmann, D.; Huth, T.; Cryns, K.; Deforce, S.; Serneels, L.; Camacho, I. E.; Marjaux, E.; Craessaerts, K.; Roebroek, A. J. M.; Schwake, M.; D'Hooge, R.; Bach, P.; Kalinke, U.; Moechars, D.; Alzheimer, C.; Reiss, K.; Saftig, P.; De Strooper, B. Phenotypic and biochemical analyses of BACE1- and BACE2-deficient mice. *J. Biol. Chem.* **2005**, *280*, 30797−30806.

(14) (a) Al-Tel, T. H.; Al-Qawasmeh, R. A.; Schmidt, M. F.; Al-Aboudi, A.; Rao, S. N.; Sabri, S. S.; Voelter, W. Rational design and synthesis of potent dibenzazepine motifs as β-secretase inhibitors. *J. Med. Chem.* **2009**, *52*, 6484−6488, and references therein. (b) Al-Tel, T. H.; Al-Qawasmeh, R. A.; Zarour, R. Design, synthesis and in vitro antimicrobial evaluation of novel imidazo[1,2-*a*]pyridine and imidazo[2,1-*b*][1,3]benzothiazol motifs. *Eur. J. Med. Chem.* **2011**, *46*, 1874−1881, and references therein.

(15) (a) Clark, D. E.; Picket, S. D. Computational methods for the prediction of drug-likeness. *Drug Discovery Today* **2000**, *5*, 49−58. (b) Kelder, J.; Grootenhuis, P. D. J.; Bayada, D. M.; Delbressine, L. P. C.; Ploemen, J. P. Polar molecular surface as a dominating determinant for oral absorption and brain penetration of drugs. *Pharm. Res.* **1999**, *16*, 1514−1519. (c) Palm, K.; Stenberg, P.; Luthman, K.; Artursson, P. Polar molecular surface properties predict the intestinal absorption of drugs in humans. *Pharm. Res.* **1997**, *14*, 568−571.

(16) Stachel, S. J.; Coburn, C. A.; Sankaranarayanan, S.; Price, E. A.; Pietrak, B. L.; Huang, Q.; Lineberger, J.; Espeseth, A. S.; Jin, L.; Ellis, J.; Holloway, M. K.; Munshi, S.; Allison, T.; Hazuda, D.; Simon, A. J.; Graham, S. L.; Vacca, J. P. Macrocyclic inhibitors of β-secretase: functional activity in an animal model. *J. Med. Chem.* **2006**, *49*, 6147−6150, and references therein.

(17) Fersht, A. *Structure and Mechanism in Protein Science: A Guide to Enzyme Catalysis and Protein Folding*, 3rd ed; W. H. Freeman: New York, 1999.

(18) (a) Jain, A. N. Surflex: fully automatic flexible molecular docking using a molecular similarity-based search engine. *J. Med. Chem.* **2003**, *46*, 499−511. (b) Jain, A. N. Virtual screening in lead discovery and optimization. *Curr. Opin. Drug Discovery Dev.* **2004**, *7*, 396−403. (c) Pham, T. A.; Jain, A. N. Parameter estimation for scoring protein−ligand interactions using negative training data. *J. Med. Chem.* **2006**, *49*, 5856−5868. (d) Jain, A. N. Surflex-Dock 2.1: robust performance from ligand energetic modeling, ring flexibility, and knowledge-based search. *J. Comput.-Aided Mol. Des.* **2007**, *21*, 281−306. (e) Jain, A. N. Bias, reporting and sharing: computational evaluations of docking methods. *J. Comput.-Aided Mol. Des.* **2008**, *22*, 201−212. (f) Jain, A. N. Effects of protein conformation in docking: improved pose prediction through protein pocket adaptation. *J. Comput.-Aided Mol. Des.* **2009**, *23*, 355−374.